Acoustic emission and microslip precursors to stick-slip failure in sheared granular material

P. A. Johnson,[1] B. Ferdowsi,[2,3] B. M. Kaproth,[4] M. Scuderi,[4] M. Griffa,[3] J. Carmeliet,[2,3] R. A. Guyer,[1] P-Y. Le Bas,[1] D. T. Trugman,[1] and C. Marone[4]

Received 29 August 2013; revised 16 October 2013; accepted 18 October 2013; published 4 November 2013.

[1] We investigate the physics of laboratory earthquake precursors in a biaxial shear configuration. We conduct laboratory experiments at room temperature and humidity in which we shear layers of glass beads under applied normal loads of 2–8 MPa and with shearing rates of 5–10 μm/s. We show that above ~3 MPa load, acoustic emission (AE), and shear microfailure (microslip) precursors exhibit an exponential increase in rate of occurrence, culminating in stick-slip failure. Precursors take place where the material is in a critical state—still modestly dilating, yet while the macroscopic frictional strength is no longer increasing.
Citation: Johnson, P. A., B. Ferdowsi, B. M. Kaproth, M. Scuderi, M. Griffa, J. Carmeliet, R. A. Guyer, P.-Y. Le Bas, D. T. Trugman, and C. Marone (2013), Acoustic emission and microslip precursors to stick-slip failure in sheared granular material, *Geophys. Res. Lett.*, *40*, 5627–5631, doi:10.1002/2013GL057848.

1. Introduction

[2] Precursors to stick-slip events are seen in the field, in laboratory experiments, and in numerical simulation. Observations of precursors to slip may prove to be important in that they may ultimately help constrain periods of increased seismic hazard. Although precursors have been observed for a significant number of earthquakes [e.g., *Bouchon et al*., 2013; *Kato et al*., 2012; *McGuire et al*., 2005; *Zanzerkia et al*., 2003; *Dodge et al*., 1996], many earthquakes apparently exhibit no precursor activity. This fact may be due to incomplete seismic catalogs, as precursors can be very small in magnitude. The question is very much open at this time [*Mignan*, 2011]; however, the recent work of *Bouchon et al*. [2013], for instance, is tantalizing in its demonstration of precursor activity for a significant number of interplate events.

[3] The results of many studies suggest that the dynamics of granular media may be key to understanding systems that exhibit stick-slip behavior [e.g., *Marone*, 1998; *Nasuno et al*., 1998; *Dalton and Corcoran*, 2001; *Johnson et al*., 2008, 2012]. For instance, in experiments involving a granular gouge sheared along a fixed direction, *Nasuno et al*. [1997] observe microscopic rearrangements in gouge material preceding slip. Accumulation of these rearrangements leads to creep, with the frequency of rearrangement rising dramatically as slip approaches. Employing a device consisting of an annular plate rotating over a granular material, *Dalton and Corcoran* [2002] observe a wide spectrum of acoustic emission (AE) patterns surrounding the timing of a stick-slip event. Acoustic emission, analogous to seismic events in the earth, is a commonly observed phenomenon leading to fracture in experiments with rock and other solids [e.g., *Berkovits and Fang*, 1995; *Hamstad*, 1986; *Roberts and Talebzadeh*, 2003].

[4] There is a growing body of numerical modeling of granular materials that has been undertaken to gain insight into both field and laboratory observations [*Ferdowsi et al*., 2013; *Griffa et al*., 2012; *Aharonov and Sparks*, 1999]. In a recent 3-D, Discrete Element Method (DEM) simulation that emulates laboratory experiments of sheared granular media, for example, *Ferdowsi et al*. [2013] report an increased rate of microslip events as a stick-slip event is approached.

[5] Here we describe laboratory measurements on sheared granular material that exhibits stick-slip behavior, allowing us to examine precursors to stick slip and to explore the controlling physics. The apparatus is the biaxial shearing apparatus of Marone and coworkers [*Marone*, 1998; *Frye and Marone*, 2002; *Boettcher and Marone*, 2004; *Anthony and Marone*, 2005; *Savage and Marone*, 2007; *Knuth*, 2011]. We begin by describing the apparatus and the experimental procedure and then show the results. We follow this with a discussion of these results and conclude.

2. Experiment

[6] We perform experiments using the biaxial testing apparatus shown in Figure 1a [e.g., *Marone*, 1998]. Two layers of simulated fault gouge, under constant normal stress, are subjected to a shear stress. The normal stress ranges from 2–8 MPa. The shear stress and friction on the gouge layers, from the center drive block and measured with a load cell, is an important experimental output. The simulated fault gouge comprises class IV spheres (dimension from 105–149 μm). The initial layer thickness is 2 × 4 mm (two layers), and the roughened interfaces with the drive block have dimensions 10 cm × 10 cm. The drive block vertical displacement rate is 5 μm/s, corresponding to a

Additional supporting information may be found in the online version of this article.

[1]Los Alamos National Laboratory, Geophysics Group, Los Alamos, New Mexico, USA.
[2]Swiss Federal Institute of Technology Zürich (ETHZ), D-BAUG, Zürich, Switzerland.
[3]Swiss Federal Laboratories for Materials Science and Technology (EMPA), Dübendorf (ZH), Switzerland.
[4]Department of Geosciences, Pennsylvania State University, University Park, Pennsylvania, USA.

Corresponding author: P. A. Johnson, Los Alamos National Laboratory, Geophysics Group, PO Box 1663, Los Alamos, NM 87545, USA. (paj@lanl.gov)

0094-8276/13/10.1002/2013GL057848

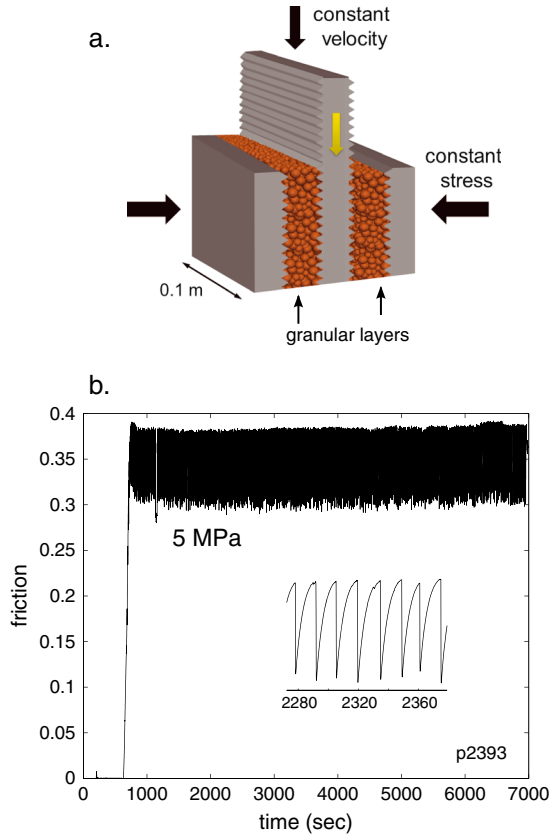

Figure 1. Experimental configuration, with measured data. (a) The biaxial shearing sample, comprised of a three block system with two layers of glass beads. The central block is driven at a constant displacement rate. The stress normal to the layers, applied as indicated by arrows, is maintained constant. (b) Complete record for a representative experiment showing friction μ $\left[\mu = \frac{F/A}{\sigma}\right]$ versus time, where σ is normal load, A is the block area and F is the applied shearing force. The data show hundreds of stick-slip events, with maximum friction of ~0.38 and friction drops of ~0.08. The inset shows an expanded view of the friction behavior. The shear rate was initially 10 μm/s for the range 0 to ~5000 μm and 5 μm/s thereafter.

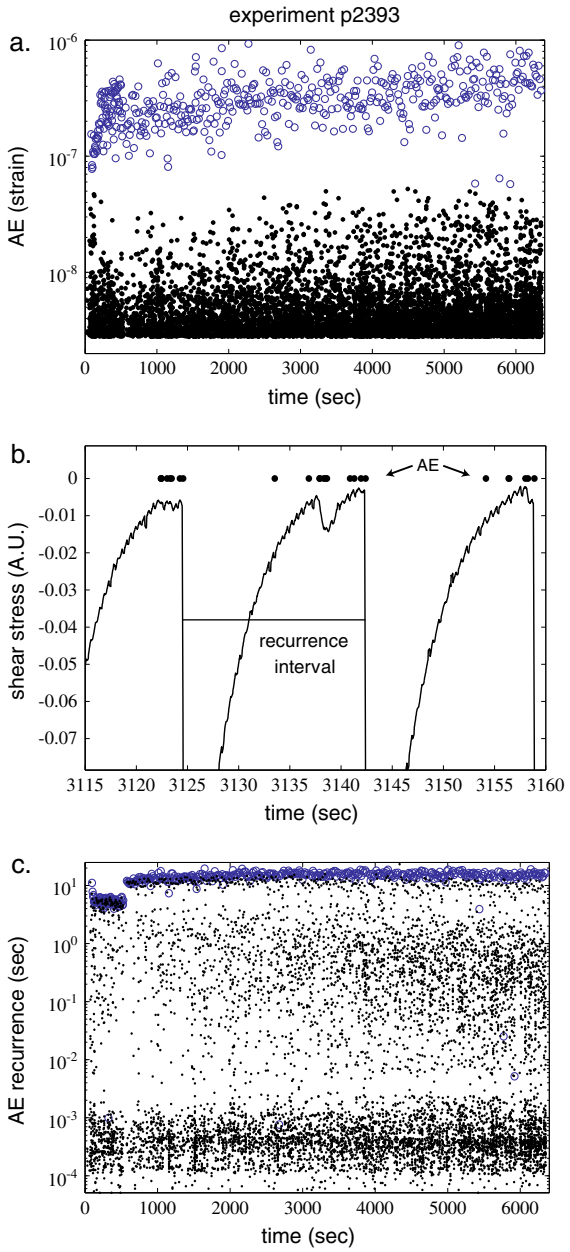

Figure 2. Acoustic emission (AE) characteristics. (a) AE amplitude as a function of time (semilog scale) from the characteristic stick-slip events (open circles) and precursor events (solid circles). The AE precursors are plotted according to their relative strain amplitude, which varies from 3×10^{-9} to 5×10^{-8}. (b) Expanded view of a portion of the experiment, showing the timing of the precursor AE (solid black circles). The solid black line is the shear stress (arbitrary units). The characteristic event recurrence interval of stick slips is noted. Precursory AEs begin late in the stick-slip cycle and are frequently (but not always) associated with microshear failures. (c) AE recurrence interval versus time (semilog scale) for the entire experiment. Large, open circles (blue) are AE from characteristic stick-slip events, and small, closed circles (black) are precursor AE. Note that the AE recurrence times for the early portion of the experiment are shorter because the shearing rate is higher for time < 500 s.

strain rate of approximately 1.2×10^{-3} /s. The apparatus is servocontrolled so that constant normal stress and displacement rate of the drive block are maintained at ±0.1 kN and ±0.1 μm/s, respectively. The apparatus is monitored via computer to record load on the drive block and drive block displacement at 10 kHz.

[7] Acoustic emission, detected on the central block via a Brüel and Kjær model 4393 accelerometer and amplified by a Brüel and Kjær 2635 charge amplifier, is a second important experimental output. From the measured acceleration, the strain ε associated with the acoustic emission is found using the particle velocity u, layer wave speed c, and particle acceleration $\ddot{u}$: $\varepsilon = \frac{\dot{u}}{c}$, where $\dot{u} = \frac{\ddot{u}}{\omega}$ and $\omega = 2\pi f$ [e.g., *Aki and Richards*, 2002]. The average measured wave speed in the granular material is $c \sim 700$ m/s, and frequency f is 40.3 kHz. After band pass filtering the signal at 34–45 kHz, we extract acoustic emissions using a thresholding algorithm in which events are identified by amplitudes that exceed a

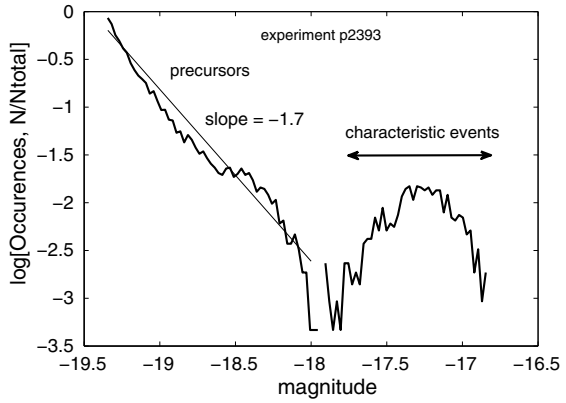

Figure 3. Relative probability of acoustic emission occurrence versus magnitude (as defined in the supporting information), plotted on a log-log scale. The emission from characteristic events, the stick slips, are noted by the double arrow. The slope of the precursor emission is denoted by the thin, solid line.

fixed strain threshold of 2.7773^{-09}. We find by visual inspection that all recorded events are captured, with the exception of misidentification of multiple events as a single event. This is rare, however. The shear microfailures termed microslips are obtained from the shear stress signal by extracting events that exceed a 0.002 MPa threshold.

3. Observations

[8] In the following, we describe the observations associated with precursor phenomena observed in the shear stress and in the acoustic emission. Figure 1b shows the shear stress as a function of time delivered by the drive block, in the form of a coefficient of friction μ (shear stress divided by the normal stress $\mu = \frac{\tau}{\sigma}$), for an experiment conducted at 5 MPa normal stress. The inset shows an expanded view of the frictional behavior. In Figure 2a, the strain of each AE event is plotted versus the time of its occurrence. The large amplitude AE events (open circles in Figure 2a) are associated with the stick-slip events in Figure 1b. The small amplitude AE events (closed circles) are precursors to the stick-slip events. This is made clear in the expanded view in Figure 2b, where the relation between acoustic emission and stick slip can be seen. The small amplitude AE events (closed circles in Figure 2a) are on average 2 orders of magnitude smaller in strain amplitude than the AE events associated with stick-slip events (open circles in Figure 2a). The small amplitude AE events occur before the stick-slip event in a time domain in which small stick-slip events (microslips) are seen (Figure 2b). Following each stick-slip event, there is a quiescent period (no microslips and no AE, see also Figure S1 of the supporting information).

[9] The probability distribution of all of the AE events, as a function of event magnitude (as defined in the supporting information), is shown in Figure 3 on a log-log scale. Such a plot is the laboratory equivalent of a Gutenberg-Richter (GR) plot [*Gutenberg and Richter*, 1954]. The AE events associated with stick slips, the *characteristic* stick-slip events, form the peak to the right and have mean magnitudes of about −17.3. The cumulative probability of precursor AE events is described approximately by $\mathrm{Log}_{10}N = a - bM$, $b \approx 1.7$. (For comparison, b for the global GR plot is 1.0). The fact that the laboratory GR plot and the global GR plot are within a factor of two provides reassurance that the laboratory system captures some of the relevant physics of faults within the earth. The relative ease of separating precursor AE events from stick-slip AE events in this laboratory experiment does not, however, carry over to the earth, where characteristic stick-slip behavior is rare.

[10] The repeatability of the stick-slip events in the laboratory experiments allows us to regard the interval between each such event as a realization of a basic mechanical evolution of the system. Thus, we construct the probability density of precursor events as a function of time measured from the moment of stick slip. We do this for the AE events in Figure 4a and for the microslips in Figure 4b. In Figure 4, at times far from the stick-slip event, we see a low, approximately uniform, background probability density for AE and microslip events. As the stick slip is approached, the AE and microslip probability density rises above the background approximately exponentially. Immediately preceding the slip there is a rapid acceleration of AE and microslips. The inset of Figure 4b shows an overlay of the two probability density functions (PDFs), normalized to their respective total

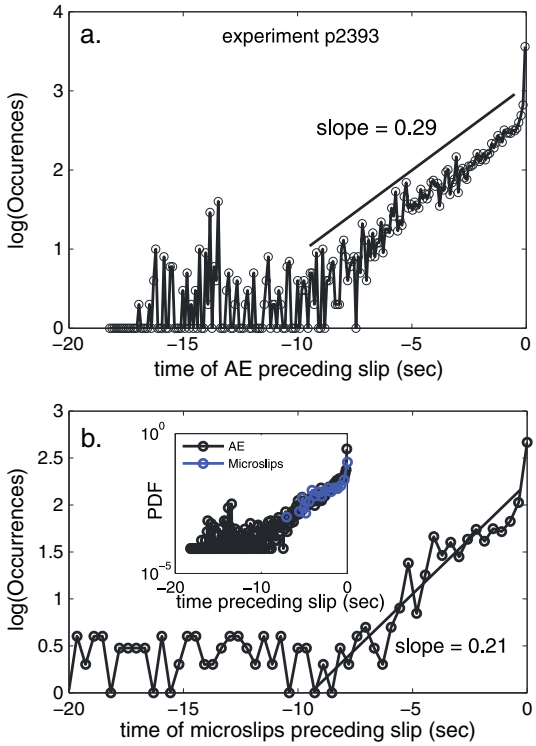

Figure 4. PDFs of the AE and microslip data. (a) Occurrence versus time plot (log-log scale) of all precursor data in experiment p2393 (excluding data from the initial shearing rate of 10 μm /s). The plot is constructed by summing as a function of time, the number of precursors preceding each stick slip. All stick slips are then set to zero time, and all data are plotted together. See supporting information for details. The slope of the exponential increase in AE activity (linear in log-log space) is noted. (b) Occurrence versus time plot (log-log scale) for microslip shear failures. The slope of the exponential increase in microslip activity (linear in log-log space) is noted. The inset shows normed AE and microslip shear failure data plotted together. The data are renormalized by their total number for the inset.

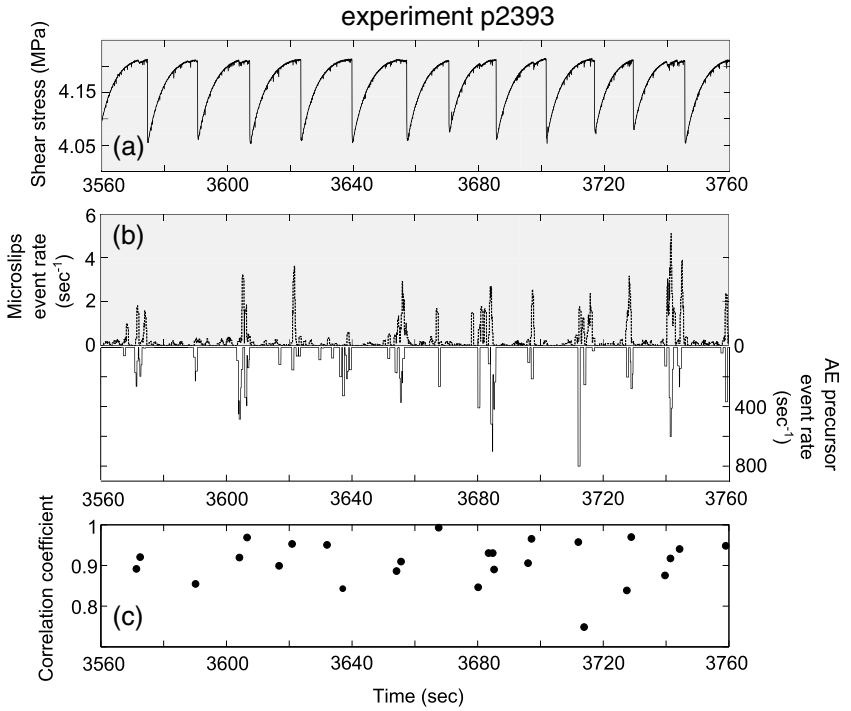

Figure 5. Correlation of microslips with AE. (a) expanded view of a portion of the shear stress signal from experiment p2393. (b) The microslip event rate (positive portion of *y* axis, shaded) and the precursor event rate (negative portion of *y* axis, unshaded), determined from the AE over the same time interval. (c) Correlation coefficients between the AE and microslip shear stress signals for each sequence leading to stick slip. See supporting information for computational details.

numbers. The slopes collapse onto each other, indicating correlation between the microslips and AE.

[11] We next determine quantitatively the relation of AE to discrete microslips. We identify 12,991 AE and 4875 microslips for 620 stick-slip events. We construct two signals (Figure 5): event rates of microslips and precursors versus time (details are available in the supporting information and in Figure S2). An expanded view of the both the AE and microslip time signals is shown in Figure 5b. There is a clear increase in both AE and microslips as characteristic slip events are approached (Figure 5a). Figure 5c shows that a cross-correlation analysis performed between the two time series gives an average correlation coefficient of 0.82, suggesting strong correlation. The results described here are for a single value of the normal stress, 5 MPa. Results for the stress range 2 MPa to 8 MPa are reported in the supporting information (see Figures S4–S7).

[12] The precursors we call attention to occur primarily in a time domain in which the shear stress delivered by the drive block to the gouge layers is very slowly increasing (Figures 2b and S3), and where both granular material dilation and slow slip are taking place. The material is approaching or is already in a critical state, near failure during this time. Displacement of the shearing block associated with individual precursors is not measureable above the background shearing rate—the gouge material weakens while simultaneously broadcasting AE, but there is no associated slip. We infer that this is due to the fact that only a portion of the gouge material fails during a precursor. In contrast, in a characteristic event, a large displacement is recorded, along with a significant shear stress decrease and large amplitude AE. Details of the workings of the shearing system over a frictional cycle are described in the supporting information (see Figure S3).

4. Analysis and Discussion

[13] It is clear from the results shown in Figures 4 and 5 that precursory AEs and microslips are associated. Most microslips exhibit AE; however, many AEs do not exhibit microslips. The signal-to-noise ratio of the AEs (about 10^3) is significantly larger than that of the microslips (about 10^2). Thus many microslips are likely missed in the analysis, and some may be so small as to exhibit no shear stress signature.

[14] The microslips are associated with grain rearrangements within the shearing layer. The DEM simulation work of *Ferdowsi et al*. [2013] shows that microslips are associated with an increase in the number of slipping contacts as well as an increase in the kinetic energy of the granular layers. In short, the grain rearrangements observed in the simulation and surmised from the experiments can be viewed as the result of bead asperities that resist the slow slip, leading to local failures that produce precursors, and eventually failing catastrophically in a stick-slip event. There is no obvious evidence of static stress transfer triggering the stick slip in the experimental data, as we observe no build up of shear load due to the AE/microslips.

[15] In summary, the experiments resemble interplate precursor activity observed in the earth and indicate that a more careful inspection of high quality data preceding interplate events may prove useful. Precursors may be very small in magnitude and therefore demand better instrumentation in earthquake prone regions.

[16] **Acknowledgments.** This work was supported by Institutional Support (LDRD) at Los Alamos to P.J., R.G., P.-Y.L.B., and D.T.T.; the Institute of Geophysics and Planetary Physics at Los Alamos to C.M., M.S., B.K., and P.J.; NSF grants OCE 0648331 and NSF-EAR0911569 to C.M., and Swiss National Science Foundation grants projects 206021-128754 and 200021-135492 to B.F., M.G., and J.C.

[17] The Editor thanks Harmony Colella and an anonymous reviewer for their assistance in evaluating this paper.

References

Aharonov, E., and D. Sparks (1999), Rigidity phase transition in granular packings, *Phys. Rev. E.*, *60*, 6890–6896, doi:10.1103/PhysRevE.60.6890.

Aki, K., and P. Richards (2002), *Quantitative Seismology*, University Science Books, Sausalito, California.

Anthony, J. L., and C. Marone (2005), Influence of particle characteristics on granular friction, *J. Geophys. Res.*, *110*, B08409, doi:10.1029/2004JB003399.

Berkovits, A., and D. Fang (1995), Study of fatigue crack characteristics by acoustic emission, *Eng. Fract. Mech.*, *51*, 401–416, doi:10.1016/0013-7944(94)00274-L.

Boettcher, M. S., and C. Marone (2004), Effects of normal stress variation on the strength and stability of creeping faults, *J. Geophys. Res.*, *109*, B03406, doi:10.1029/2003JB002824.

Bouchon, M., V. Durand, D. Marsan, H. Karabulut, and J. Schmittbuhl (2013), The long precursory phase of most large interplate earthquakes, *Nat. Geosci.*, *6*, 299–302, doi:10.1038/NGEO1770.

Dalton, F., and D. Corcoran (2001), Self-organized criticality in a sheared granular stick-slip system, *Phys. Rev. E*, *63*, 061312, doi:10.1103/PhysRevE.63.061312.

Dalton, F., and D. Corcoran (2002), Earthquake behaviour and large-event predictability in a sheared granular stick-slip system, *arXiv preprint physics/0211060*.

Dodge, D. A., G. C. Beroza, and W. Ellsworth (1996), Detailed observations of California foreshock sequences: Implications for the earthquake initiation process, *J. Geophys. Res.*, *101*, 22,371–22,392, doi:10.1029/96JB02269.

Ferdowsi, B., M. Griffa, R. A. Guyer, P. A. Johnson, C. Marone, *and* J. Carmeliet (2013), Microslips as precursors of large slip events in the stick-slip dynamics of sheared granular layers: A discrete element model analysis, *Geophys. Res. Lett.*, *40*, 4194–4198, doi:10.1002/grl.50813.

Frye, K. M., and C. Marone (2002), Effect of humidity on granular friction at room temperature, *J. Geophys. Res.*, *107*(B11), 2309, doi:10.1029/2001JB000654.

Griffa, M., B. Ferdowsi, E. Daub, R. Guyer, P. Johnson, C. Marone, and J. Carmeliet (2012), Meso-mechanical analysis of deformation characteristics for dynamically triggered slip in a granular medium, *Philos. Mag.*, *92*, 3520–3539, doi:10.1080/14786435.2012.700417.

Gutenberg, B., and C. Richter (1954), *Seismicity of the Earth and its Associated Phenomena*, Princeton University Press, Princeton, NJ.

Hamstad, M. A. (1986), A review: Acoustic emission, a tool for composite-materials studies, *Exp. Mech.*, *26*, 7–13, doi:10.1007/BF02319949.

Johnson, P., H. Savage, M. Knuth, J. Gomberg, and C. Marone (2008), The effect of acoustic waves on stick-slip behavior in sheared granular media: Implications for earthquake recurrence and triggering, *Nature*, *451*, 57–60, doi:10.1038/nature06440.

Johnson, P., B. Carpenter, M. Knuth, B. Kaproth, P. Le Bas, E. Daub, and C. Marone (2012), Nonlinear dynamical triggering of slow slip on simulated earthquake faults with implications to Earth, *J. Geophys. Res.*, *117*, B04310, doi:10.1029/2011JB008594.

Kato, A., K. Obara, T. Igarashi, H. Tsuruoka, S. Nakagawa, and N. Hirata (2012), Propagation of slow slip leading up to the 2011 Mw 9.0 Tohoku-Oki earthquake, *Science*, *335*, 705–708, doi:10.1126/science.1215141.

Knuth, M. W. (2011), Ultrasonic velocity measurements in sheared granular layers: Implications for the evolution of dynamic elastic moduli of compositionally-diverse cataclastic fault gouges, PhD thesis, University of Wisconsin - Madison.

Marone, C. (1998), Laboratory-derived friction laws and their application to seismic faulting, *Annu. Rev. Earth Planet. Sci.*, *26*, 643–696.

McGuire, J. J., M. S. Boettcher, and T. H. Jordan (2005), Foreshock sequences and short-term earthquake predictability on East Pacific Rise transform faults, *Nature*, *434*, 457–461, doi:10.1038/nature03377.

Mignan, A. (2011), Retrospective on the Accelerating Seismic Release (ASR) hypothesis: Controversy and new horizons, *Tectonophysics*, *505*, 1–15, doi:10.1016/j.tecto.2011.03.010.

Nasuno, S., A. Kudrolli, and J. P. Gollub (1997), Friction in granular layers: Hysteresis and precursors, *Phys. Rev. Lett.*, *79*, 949–952, doi:10.1103/PhysRevLett.79.949.

Nasuno, S., A. Kudrolli, A. Bak, and J. P. Gollub (1998), Time-resolved studies of stick-slip friction in sheared granular layers, *Phys. Rev. E.*, *58*, 2161–2171, doi:10.1103/PhysRevE.58.2161.

Roberts, T. M., and M. Talebzadeh (2003), Acoustic emission monitoring of fatigue crack propagation, *J. Construct. Steel Res.*, *59*, 695–712, doi:10.1016/S0143-974X(02)00064-0.

Savage, H. M., and C. Marone (2007), Effects of shear velocity oscillations on stick-slip behavior in laboratory experiments, *J. Geophys. Res.*, *112*, B02301, doi:10.1029/2005JB004238.

Zanzerkia, E. E., G. C. Beroza, and J. E. Vidale (2003), Waveform analysis of the 1999 Hector Mine foreshock sequence, *Geophys. Res. Lett.*, *30*(8), 1429, doi:10.1029/2002GL016383.